

An experiment on the dynamics of thermal diffusion

M. C. Sullivan and B. G. Thompson^{a)}

Department of Physics, Ithaca College, Ithaca, New York 14850

A. P. Williamson

Martin Fisher School of Physics, Brandeis University, Waltham, Massachusetts 02454

(Received 30 July 2007; accepted 5 February 2008)

We present an experiment that demonstrates thermal diffusion in metals via a dynamic measurement of the temperature in a metal rod as a function of position and time. From this single measurement and using simple heat flow equations, we can extract the thermal conductivity and the specific heat of the metal to within 5% of the accepted values. This experiment can be extended for advanced students, who can model the heat flow by including heat losses and finite heater models via a numerical solution of a partial differential equation. © 2008 American Association of Physics Teachers.

[DOI: 10.1119/1.2888544]

I. INTRODUCTION

So much attention is paid to wave phenomena in introductory physics that it is easy to shortchange other energy transport phenomena. This paper describes an experiment where the temperature of a metal rod is measured at several points after a pulse of heat is applied. The experiment illustrates the dynamics of thermal diffusion and measures the thermal conductivity and heat capacity of the material simultaneously. Although others have described experiments involving thermal diffusion,^{1–10} this experiment is useful for undergraduates because it is dynamic, measures two important material properties in one experiment, provides easy visualization of the phenomenon from the data plot, exposes students to a partial differential diffusion equation, surprises students when the Gaussian exponential arises in a new context as a solution, and is low cost, excluding common laboratory equipment such as computerized data acquisition. It can be extended to include the use of numerical methods to solve a partial differential equation.

The experiment was first described by Kuckes and Thompson.^{11,12} Although the original apparatus provided a qualitative illustration of the phenomenon, the quantitative determination of the material constants was poor and inconsistent. This paper describes improvements to the apparatus and analysis, which lead to estimates of the parameters to within 5% of the accepted values.

We begin with a description of the apparatus and a review of the theory of a heat pulse in a rod. The limitations of the original results are then discussed together with improvements to the analysis. We then discuss changes to the apparatus and experimental procedure, which result in consistent and expected values of the thermal conductivity and heat capacity. Example datasets are provided for copper and gold, and other materials are considered.

II. APPARATUS AND PROCEDURE

The apparatus suggested in Refs. 11 and 12 consists of a 3.2 mm diameter copper rod approximately 15 cm long with a 3.3 Ω heater resistor at one end and thermistors attached to the rod at distances of 2.5 and 5.1 cm from the heater. The end of the rod opposite the heater is attached to an aluminum plate, which acts as a heat sink. A glass jar is placed over the rod to reduce the heat loss due to air drafts and radiation. Each thermistor is attached to a variable resistor to make a

voltage divider, the voltage from which is amplified by an op-amp circuit. The output voltage of the circuit is measured by a computerized data acquisition system.¹³ The computer also controls the power to the heater through a transistor switch. The voltage amplifier and switch are described in more detail in Appendix A.

The heater provides a point source of heat in the rod over a short interval of time. This heat pulse is delivered by a current pulse of about 1 A in the resistor with a duration of 0.1 to 1.0 s controlled by a computer. After the pulse, the computer measures the voltage outputs of the thermistor op-amps over about 60 s. Before starting a run, the trimpot for each thermistor voltage divider should be adjusted so that the output voltage of the amplifier is slightly above zero. This procedure ensures that the op-amp is in its active region. Significant changes in the temperature happen quickly so the sample rate should be at least 10 s⁻¹. Before the next run, we let the rod cool until the temperature stabilizes and readjust the trimpot. Additionally, we measure the voltage across the heater resistance with the power applied so that the total input energy can be calculated.

After a run the computer subtracts the initial offset voltage and applies the calculated gain factor to obtain the temperature change in Kelvin as a function of time. The amplifier gain calculation and temperature conversion is described in detail in Appendix A. The computer should also subtract an appropriate time difference so that time is measured from the midpoint of the pulse to ensure that the data can be compared to the model.¹²

III. SYSTEM MODEL AND DATA ANALYSIS

The primary model for this experiment is the transport of heat in an infinite rod due to a point source of energy in the middle.^{12,14} The transport of heat along the rod follows the one-dimensional diffusion equation

$$s \frac{\partial \Theta}{\partial t} = \kappa \frac{\partial^2 \Theta}{\partial z^2}, \quad (1)$$

where $\Theta = \Theta(z, t)$ is the temperature change of the rod with respect to the equilibrium temperature, κ is the thermal conductivity, and s is the volumetric heat capacity (the specific heat c multiplied by the density ρ). The equilibrium temperature is assumed to be the ambient temperature of the air at the start, T_a . Therefore, $\Theta(z, t) = T_r(z, t) - T_a$, where $T_r(z, t)$ is

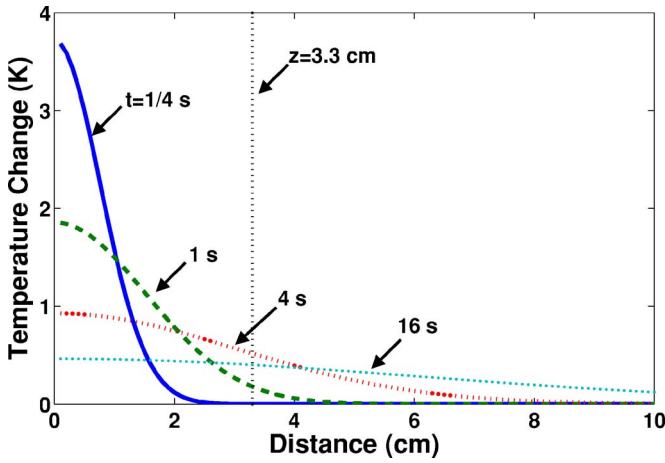


Fig. 1. (Color online) The temperature change as a function of distance along a 3.2 mm diam. copper rod for times $t=0.25, 1, 4,$ and 16 s. The profile is a Gaussian in the distance z and decreases in amplitude and increases in width with increasing time. At the point along the rod indicated by the vertical line at $z=3.3$ cm, the temperature first increases, then slowly decays back to zero temperature change.

the temperature of the rod as a function of position and time.

The solution for a heat pulse Q at the center of the rod is

$$\Theta = \frac{Q}{2A\sqrt{\pi\kappa st}} e^{-z^2/4\kappa t}, \quad (2)$$

where $A = \pi a^2$ is the cross-sectional area of the rod with radius a . By symmetry the solution for a half infinite rod, where all of the heat goes in one direction, is the same as Eq. (2), but with twice the temperature change. Note that the solution is a Gaussian function of distance whose height decreases and whose width increases in time. The temperature change as a function of position given by Eq. (2) for several times after the pulse of heat is shown in Fig. 1. The contrast with the solution of the wave equation is clear; the heat pulse does not travel along the rod like a wave. However, the temperature at a particular distance (the vertical line in Fig. 1) will first rise and then fall, as if a pulse had passed by.

For measurements of the temperature change Θ for the infinite rod as a function of time at a particular position, z , the solution can be written in terms of the characteristic time t_c and characteristic temperature change Θ_c :

$$\Theta = \Theta_c \sqrt{\frac{t_c}{t}} e^{-t/t_c}, \quad (3)$$

where $t_c = z^2/4\kappa$ and $\Theta_c = Q/Az\sqrt{\pi}$.¹² The characteristic time and temperature change are related to the time and temperature change at the peak in the curve: $t_{\text{peak}} = 2t_c$ and $\Theta_{\text{peak}} = \sqrt{1/2e}\Theta_c \approx 0.43\Theta_c$. Therefore, a first estimate of s is obtained by determining the peak temperature change. Knowing s , the thermal conductivity κ is determined from the time of the peak. A finite time pulse can be accurately modeled by this pulse solution provided that the time is measured from the center of the finite time pulse and the pulse duration is $\lesssim 0.5t_c$, or roughly less than 1 s for copper when $z \approx 2.5$ cm.¹²

Typical results from a 3.2 mm diameter copper rod at two distances for a 0.5 s pulse of heat are shown in Fig. 2 together with the models generated from the time and height of the peaks. Note that the models fit well at early times for

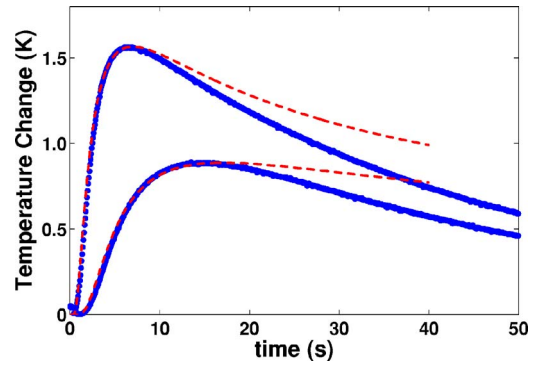


Fig. 2. (Color online) Observed temperatures (solid lines) in a 3.2 mm diameter copper rod as a function of time at distances from the heater of 2.5 cm (upper curve) and 5.1 cm (lower curve). The model (dashed lines) fits well at early times, but greatly underestimates the heat losses for larger times. The fitting parameters required to achieve good fits for the two thermistors are different.

each distance taken individually. They do not fit well when the constants obtained from the data from one thermistor are used to generate the model for the second thermistor. The constants obtained from these curves also deviate from accepted values by roughly 20%. At later times, the temperature falls more rapidly than the model predicts, possibly skewing the peak toward lower temperature changes and shorter times. We conclude that this experiment gives qualitative agreement with the predictions of Eq. (3), but can be dissatisfying because students do not obtain consistent results or results that agree with expected values.

IV. IMPROVED ANALYSIS

One change in the analysis procedure can bring consistency between the models at the two distances. The original heater was a 3.3 Ω metal film resistor that was embedded using heat conductive epoxy in a short length of copper rod that was soldered to the end of the thermistor rod. The heat conductance of the epoxy and the resistor body are much less than those of the rod. Because the heater does not heat a small volume uniformly, and the heat is moving out of the heated area more slowly, the effective distance from the heater to the measurement position is more than the measured distance.

We can account for this additional distance by adding an effective distance z_{eff} to each thermistor distance, such that $z = z_{\text{measured}} + z_{\text{eff}}$. Note that s depends on the inverse of z and κ depends linearly on z , so adding this effective distance does not simply scale the solutions. The data at the two distances can now be fitted by adjusting three parameters, s , κ , and z_{eff} . A model with $z_{\text{eff}} \approx 9$ mm fits the data from both thermistors and produces similar values of s and κ . These values of s and κ are within 20% and 12% of the accepted values, respectively. Therefore, the addition of z_{eff} has ameliorated the problem of inconsistency between the parameters obtained at two distances at the cost of another fitting parameter. Qualitatively, the experimental values of s , κ , and z_{eff} , when used with Eq. (3), produce a graph very similar to Fig. 2; that is, the experiment and model agree well up to the peak, but the model underestimates the heat loss at longer times.

From the later time data it is clear that the rod is losing heat by means other than conduction down the rod. Losses

out the side of the rod to the air can be conductive, convective, or radiative. Because the coefficient of thermal conductivity of air is 10^{-4} times smaller than that of copper,¹⁵ direct conductive loss to the air is negligible. The convective transfer of heat over a time Δt is given by Fourier cooling, $\Delta Q_c = h_c A_s \Theta \Delta t$, where h_c is the convective heat transfer coefficient, and $A_s = 2\pi a \Delta z$ is the surface area of the section of the rod of length Δz and radius a .⁵

Radiative heat transfer is given by $\Delta Q_r = \epsilon \sigma A_s (T_r^4 - T_a^4) \Delta t$, where σ is the Stefan–Boltzmann constant ($5.67 \times 10^{-8} \text{ Wm}^{-2} \text{ K}^{-4}$) and ϵ is the emissivity of the surface.¹⁶ For small temperature differences, as is the case in this experiment, the radiative transfer can be written as $\Delta Q_r = 4\epsilon \sigma A_s T_a^3 \Theta \Delta t$. The overall heat loss to air for a section of rod Δz can be written as

$$\Delta Q_{\text{total}} = 2\pi a h \Delta z \Theta \Delta t, \quad (4)$$

with $h = h_c + 4\epsilon \sigma T_a^3$. The coefficient of convective heat transfer h_c is highly variable. Typical values for a vertical surface in otherwise still air are between 5 and $35 \text{ Wm}^{-2} \text{ K}^{-1}$.¹⁷ For comparison, the value of the radiative factor, $4\epsilon \sigma T_a^3$, is $6 \text{ Wm}^{-2} \text{ K}^{-1}$ at room temperature. However, the emissivity for metals with a semipolished surface is generally less than 5% .¹⁶ Also, the addition of a glass enclosure will reflect the radiative heat energy so that the effective temperature difference will not be as large as $T_r - T_a$. Both the low emissivity of metals and a reflective glass enclosure will further reduce the radiative heat loss component of the total heat loss.

This total alternate heat loss h adds another term to the partial differential equation in Eq. (1),

$$s \frac{\partial \Theta}{\partial t} = \kappa \frac{\partial^2 \Theta}{\partial z^2} - w \Theta, \quad (5)$$

where $w = 2h/a$. Although it is not obvious, Eq. (5) is soluble analytically with the addition of a time exponential to Eq. (2):

$$\Theta = \frac{Q}{2A\sqrt{\pi\kappa s t}} e^{-z^2/4\kappa t} e^{-wt/s}. \quad (6)$$

By appropriate adjustment of the parameters s , κ , w , and z_{eff} , the model can be fitted to the experimental data. Because the parameters do not have independent effects on the shape of the model curve, the fit must be done by an iterative process. A good fit is obtained over the whole time span with this analytic solution. Figure 3 shows the solution generated by Eq. (6) using accepted values of κ and c (see Table I) and $z_{\text{eff}} = 20 \text{ mm}$ and $h = 27 \text{ Wm}^{-2} \text{ K}^{-1}$. This convective heat transfer value is consistent with the range noted previously. As expected, the heat loss skews the peak temperature change and the time of the peak. Estimates of κ and c without consideration of this effect will thus be biased.

Further analysis could include the effect of adding heat to the rod over a finite period of time and over a finite distance. Adding a heat source that is not a delta function leads to an equation of the form

$$s \frac{\partial \Theta}{\partial t} = \kappa \frac{\partial^2 \Theta}{\partial z^2} + v - w \Theta, \quad (7)$$

where $v = v(z, t)$ is the power density input (energy per volume per time) for each segment of the rod. Thus, the power of the heat source could be specified over a finite region for a finite time duration and set to zero for the rest of the rod.

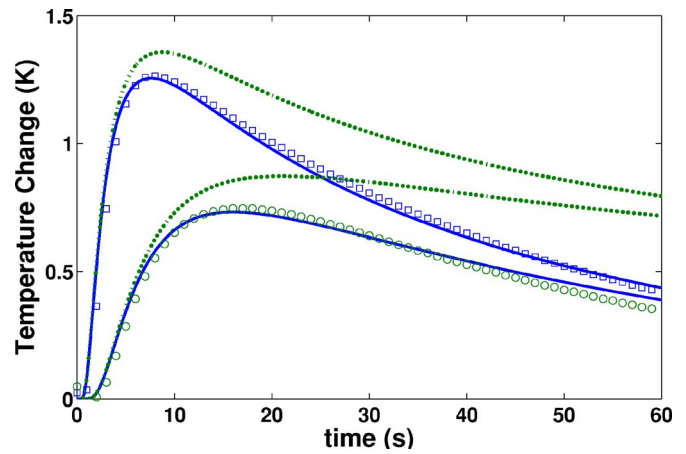


Fig. 3. (Color online) Observed temperatures in a 3.2 mm diameter copper rod as a function of time at two distances from the heater along a copper rod 2.5 cm (boxes) and 5.1 cm (circles). The solid line shows the analytical solution to Eq. (6) using κ and c from Table I and with $z_{\text{eff}} = 20 \text{ mm}$ and $h = 27 \text{ Wm}^{-2} \text{ K}^{-1}$. The dotted line is the solution without consideration of the heat loss from the sides of the rod.

For this case no analytical solution exists, and a numerical solution is necessary. Appendix B describes a procedure for a numerical solution of this equation.¹⁸

V. IMPROVED APPARATUS AND PROCEDURE

The model we have described requires four parameters to fit the data. Wouldn't it be better to fix the problems experimentally?

A metal-film resistor epoxied to the end of the rod works well for a qualitative analysis, but because we have a poor understanding of how the resistor actually heats the rod, we are forced to introduce the z_{eff} parameter to model how heat is transported from the resistor into the rod. We can reduce z_{eff} by improving the heat transfer from the heat source into the metal rod. We replaced the heater resistor with about 20 turns of 0.16 mm diameter (34 gauge) coated phosphor bronze wire wrapped directly around the rod ($R \approx 4 \Omega$) and held in place using a thin coating of thermal epoxy (Fig. 4). This heater arrangement ensures that the heat from the wire goes directly into the rod with only a minimum of uncertainty in the location and time.

We can also limit the effect of a finite size heater by moving the thermistor positions farther away. The farther the distance from the heater, the more the finite heat pulse looks like a delta function in z and t . Because the heat pulse looks more like a delta function, z_{eff} is a smaller correction to the position of the thermistors. To move the thermistors away

Table I. Thermal material properties for copper, gold, aluminum, and silver, where κ is the thermal conductivity, c is the specific heat, ρ is the density, s is the volumetric heat capacity, and α is the diffusivity (Ref. 15).

	κ (W/m-K)	c (J/kg-K)	ρ (kg/m ³)	$s = c\rho$ (J/m ³ -K)	$\alpha = \kappa/s$ (m ² /s)
Cu	401	385	8960	3.45×10^6	1.17×10^{-4}
Au	317	129	19 300	2.49×10^6	1.27×10^{-4}
Al	237	904	2700	2.44×10^6	0.97×10^{-4}
Ag	429	236	10 500	2.48×10^6	1.73×10^{-4}

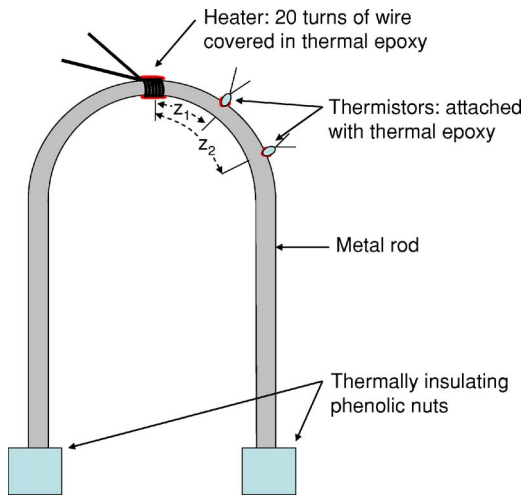


Fig. 4. (Color online) Schematic of the improved thermal diffusion apparatus. A 3.2 mm diameter, 80 cm long metal rod is bent into a U-shape. The heater is roughly 20 turns of 0.16 mm diameter (34 gauge) coated phosphor bronze wire wound directly around the rod and held in place with thermal epoxy. The thermistors are attached with thermal epoxy at $z_1=5.1$ cm and $z_2=10.2$ cm from the heater. The rods terminate in thermally insulating phenolic blocks.

from the heat source requires a longer metal rod. We use an 80 cm copper rod bent into an upside-down U shape. Using a longer rod allows us to place the heater in the center of the rod and move the thermistor positions to 5.1 cm and 10.2 cm from the heater (Fig. 4).

Moving the thermistors farther from the heat source also means that the measured temperature changes are smaller. Thus, extraneous heat sources conducted through the base plate become more influential on the temperature of the rod. To reduce their effect we used a thermal insulator instead of using a thermal sink for the rod, creating a thermally floating rod. We threaded the ends of the rod and screwed phenolic nuts (fabricated in our shop) onto them. We then secured the nuts to a brass plate. These phenolic nuts ensured that temperature changes in the brass plate were not communicated to the thermistors, and that the temperature changes measured by the thermistors came from the heater.

The fourth parameter, w , comes from the need to include heat losses. As we have argued, the heat loss at room temperature due to convection is a large percentage of the total heat loss. We eliminated most convective heat losses by operating the apparatus in a vacuum, using a diffusion pump, a bell jar, and electric feedthroughs. The data taken in air compared with data taken in a vacuum provide students with striking visual evidence of the heat loss due to convection. Figure 5 shows data taken at atmospheric pressure and in a vacuum ($P \approx 1 \times 10^{-6}$ Torr) over a 10 min time span. As expected, the temperature decays much more slowly in a vacuum. Model curves generated using Eq. (3) with accepted values for the specific heat and thermal conductivity of copper fit these data quite well (see Fig. 6). The remaining discrepancy is most likely due to a remaining radiative component of the heat loss and the rod's finite length and thermal isolation. By using the combination of improved apparatus and operation in a vacuum, we are able to model both thermistors using the same modeling parameters.

With $z_{\text{eff}}=0$, we find s and κ to within 10% of the accepted values. With a small effective distance ($z_{\text{eff}} \approx 2$ mm), we can

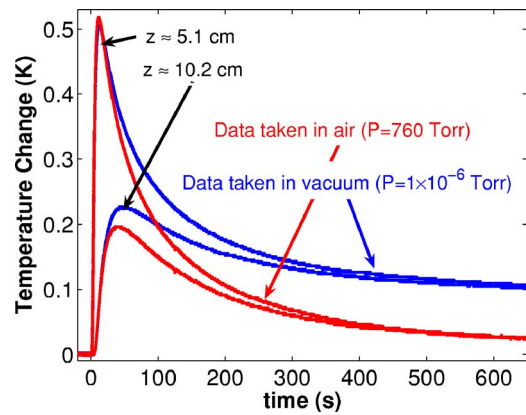


Fig. 5. (Color online) Data taken from the improved thermal diffusion apparatus. Two runs are shown for each of the thermistors at distances 5.1 cm (the two upper curves) and 10.2 cm (the two lower curves). The first run is at atmospheric pressure ($P=760$ Torr) and the second is at $P=1 \times 10^{-6}$ Torr. The data taken in air show much faster decays back to zero. For $P=1 \times 10^{-6}$ Torr the heat loss due to convection is removed, and the data decay much slower. The steps in the later time data are due to the digitization of the amplifier output voltage. The pulse time was 0.6 s and the total heat input was $Q=2.9$ J.

reduce the error to find material parameters that agree with accepted values to within 5%. A value of z_{eff} of this magnitude can be explained qualitatively as the extra distance that the heat must travel from the surface where the heat is applied to the center of the rod.

VI. CONCLUSIONS AND CHALLENGES

We have discussed a simple and inexpensive laboratory apparatus and analysis that can quickly and easily measure the heat capacity and the thermal conductivity of metals. In addition to its other advantages, this experiment demonstrates nonwave energy transport phenomena, which is often overlooked in introductory (and advanced) physics courses. We were able to measure c and κ to within 5% of the expected values.

We also discussed improvements on the original thermal diffusion experiment. Our results show that improvements to

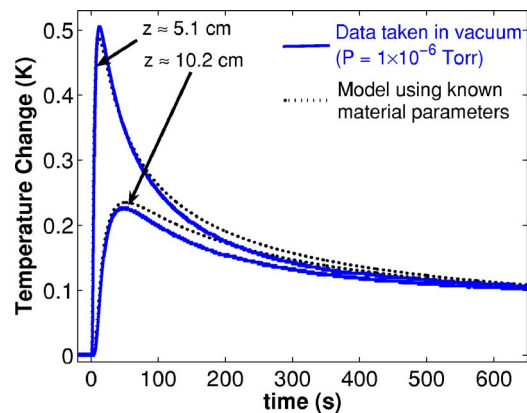


Fig. 6. (Color online) Thermal diffusion data taken with a copper rod with $P=1 \times 10^{-6}$ Torr. The data are from thermistors at 5.1 cm and 10.2 cm. The dotted lines are models using accepted material parameters for copper (see Table I) using Eq. (3) with $z_{\text{eff}}=2.5$ mm. Although some discrepancies remain, this graph shows excellent agreement between theory and experiment.

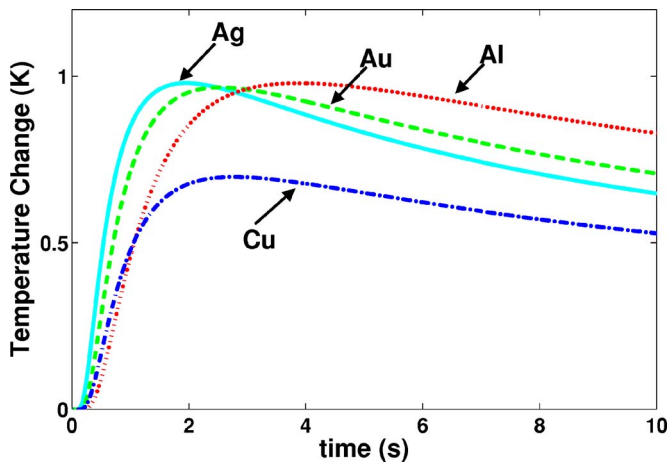


Fig. 7. (Color online) Temperature change as a function of time in a 3.2 mm diam. rod at 2.5 cm from the heat pulse for various materials, using the material parameters in Table I.

an experiment can be approached by improving the analysis or improving the experiment. An improved analysis can help us to understand inconsistencies in the data or the previous analysis. In this case, consideration of alternate heat losses allowed us to improve the fit to the data. An improved experimental apparatus and procedures can be devised to eliminate the inconsistencies and reduce errors. For this experiment a modified apparatus and procedures allowed us to reduce heat losses before analysis. It is fortunate, as in this experiment, when both approaches lead to the same understanding of the system.

Our work also suggests future challenges. To find c and κ more accurately we suggest that readers use the numerical solution to model the fact that the heater is of finite size and the heat pulse has finite duration. We also suggest that using thermally reflective surfaces and thermally absorptive surfaces in air and in vacuum can isolate the convective and radiative components of h to verify the emissivity of copper, as well as the value of the total heat loss of the system (we found $h \approx 27 \text{ Wm}^{-2} \text{ K}^{-1}$).

Finally, although copper is inexpensive, we need not limit ourselves to this metal, and the experiment can easily be adapted to other materials. Table I shows the accepted significant materials properties for several other metals.¹⁵ Figure 7 shows the predicted behavior for these when used in this experiment. In addition to the data for a copper rod, a dataset taken with a gold rod is included in Ref. 19 for students to model. Our final challenge is to adapt this experiment to measure the heat capacity and thermal conductivity of nonmetallic materials, for example, silicon, sapphire, or quartz.

ACKNOWLEDGMENTS

The authors thank A. F. Kuckes for his work on the early development of the experiment and the editors and reviewers for their suggested improvements. The authors also acknowledge the support of the Ithaca Fund of Ithaca College.

APPENDIX A: ELECTRONIC CIRCUIT DETAILS

To measure the temperature of the rod, we use a Honeywell 111-202CAK-H01 (formerly Fenwall GB32J2) ther-

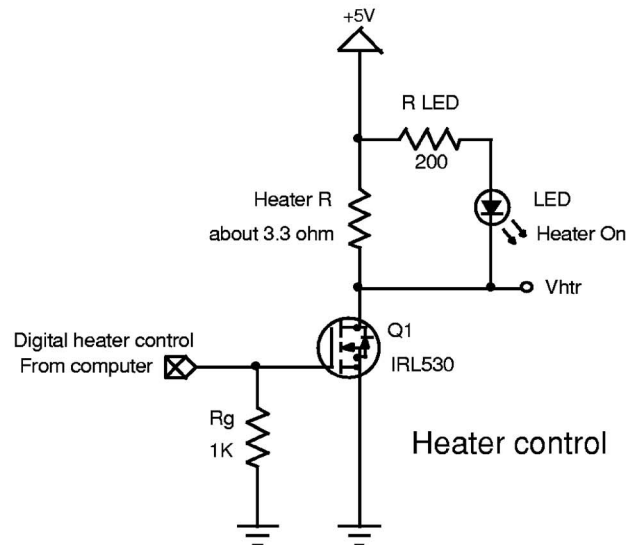
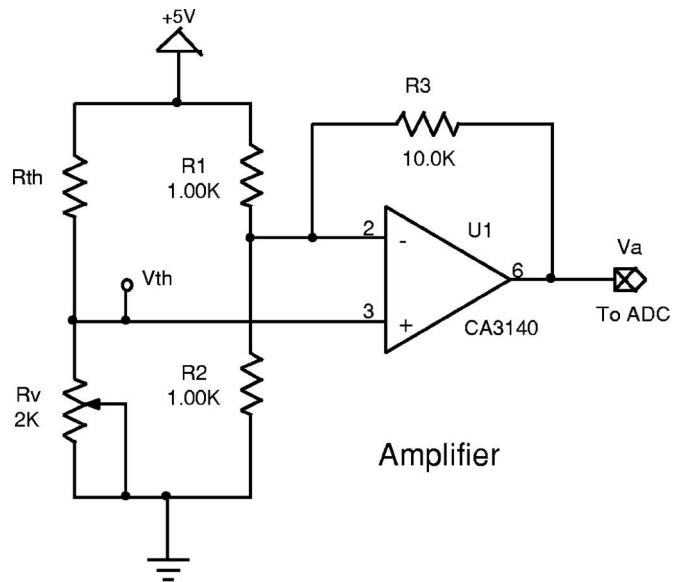


Fig. 8. Circuitry for the thermal diffusion experiment. The upper circuit schematic shows the voltage divider and amplifier for the thermistors (one for each thermistor is required). With the resistors shown, the gain is 21 for voltages at pin 3 (V_{th}). The lower schematic shows the computer control circuit for the heater. Current will flow through the heater for a +5 V control signal and will not flow for 0 V.

mistor, which has a resistance of about $2 \text{ k}\Omega$ at room temperature. The thermistor is small, and so its response time to changes in the temperature is on the order of 0.1 s. A voltage divider is constructed using the thermistor, R_{th} , and a trimpot, R_v , as shown in Fig. 8. The output of the voltage divider is

$$V_{th} = V_0 \frac{R_v}{R_{th} + R_v}, \quad (\text{A1})$$

where V_0 is the reference voltage. In our circuit V_0 is 5.0 V nominal and should be measured carefully. Because the voltage changes are small, we can write

$$dV_{th} = -V_0 \frac{dR_{th}}{R_v} \left(\frac{1}{1 + R_{th}/R_v} \right)^2. \quad (\text{A2})$$

The trimpot is adjusted before a run so that the output of the op-amp is approximately zero, which means that the $V_{th} \approx 1/2 V_0$ and thus $R_{th} \approx R_v$. Therefore

$$dV_{th} = -V_0 \frac{dR_{th}}{4R_v} \quad (A3)$$

The change in the output voltage of the op-amp circuit²⁰ is given by

$$dV_A = GdV_{th}, \quad (A4)$$

where G is the gain. For the circuit shown in Fig. 8 the gain is 21.

The thermistor resistance varies exponentially with temperature, $R_{th} = R_0 e^{T_0/T_{th}}$, where T_{th} is the absolute temperature of the thermistor, T_0 is the temperature of the semiconductor gap ($T_0 = 3440$ K for this thermistor), and R_0 is the resistance at T_0 . (The value of R_0 is not needed for this analysis.) For small resistance changes

$$dR_{th} = -R_{th} \frac{T_0}{T_{th}} \frac{dT_{th}}{T_{th}} \quad (A5)$$

Because the thermistor temperature does not change much, we can make the approximation that it is equal to the room air temperature, $T_{th} \approx T_a$. If we combine Eqs. (A3), (A5), and (A4), we see that

$$dT_{th} = T_a \frac{4}{G} \frac{T_a}{T_0} \frac{dV_A}{V_0}, \quad (A6)$$

which allows us to convert the measured voltage change to a temperature difference.

The heater control circuit uses a transistor²¹ as a switch to control the current through the heater resistance and to turn on an LED indicator. A +5 V signal from the computer turns on the current flow and a 0 V signal turns it off. The voltage across the heater resistance, $\Delta V_{hr} = 5.0 \text{ V} - V_{hr}$, should be measured when the current is flowing in order to calculate the amount of heat that is delivered to the rod, $Q = \Delta t_{hr} \Delta V_{hr}^2 / R_{hr}$, where Δt_{hr} is the duration of the heat pulse.

APPENDIX B: NUMERICAL SOLUTION FOR A FINITE HEAT PULSE

MATLAB²² has a built-in partial differential equation solver `pdepe` that can be used with equations of the form

$$g \frac{\partial u}{\partial t} = z^{-m} \frac{\partial}{\partial z} [z^m f] + j, \quad (B1)$$

where f , g , and j are functions: $f = f(z, t, u, \partial u / \partial z)$, $g = g(z, t, u, \partial u / \partial z)$, and $j = h(z, t, u, \partial u / \partial z)$. By letting $u = \Theta$, $m = 0$, $f = \kappa \partial \Theta / \partial z$, $g = s$, and $j = v - wu = v - w\Theta$, this solver is appropriate for Eq. (7). These identifications are communicated to `pdepe` using an external function. For the case of the rod with a heater in the center generating a constant power P over a period of time t_{hr} , $v = P$ for $-z_{hr}/2 < z < +z_{hr}/2$ and $0 < t < t_{hr}$ and $v = 0$ for all other positions and times.

The initial conditions and boundary values are communicated via additional functions. The initial condition is the specification of the initial values of the temperature change at each spacial grid point. For the case of Eq. (7), $\Theta = 0$ for all z because no heat has yet been added at $t = 0$.

The code requires that boundary conditions must be expressible in the form $p + qf = 0$, where p and q are functions. The boundary conditions for the infinite rod are that the ends of the rod do not experience a temperature change; that is, $\Theta = 0$ at $z = -L/2$ and $z = L/2$, where L is the (long) length of the rod. Thus, letting $p = \Theta$ and $q = 0$ will specify appropriate boundary conditions provided L is set to a large enough value for the time span considered. These boundary conditions are also appropriate for a rod whose ends are connected to a heat sink. Thus, the effect of a finite length rod can be modeled.

A mesh for the position z and also another for the time t must be specified. Because most of the dynamics take place at early times and near the heater, we used a logarithmic grid for both time and distance in order to have accurate heater models. Further details can be found in the example code provided on EPAPS¹⁹ and in the MATLAB documentation.

^aElectronic mail: bthompso@ithaca.edu

¹CENCO, Selective experiments in physics – Thermal conductivity (1940).

²E. A. Olszewski, “From baking a cake to solving the diffusion equation,” *Am. J. Phys.* **74**, 502–509 (2006).

³M. A. Karis and J. E. Scherschel, “Modelling heat flow in a thermos,” *Am. J. Phys.* **71**, 678–683 (2003).

⁴W. H. Hubin, “A course in computer-based data acquisition,” *Am. J. Phys.* **70**, 80–85 (2002).

⁵C. T. O’Sullivan, “Newton’s law of cooling – A critical assessment,” *Am. J. Phys.* **58**, 956–960 (1990).

⁶C. J. Stigter, Y. B. Mjunga, and J. M. Waryoba, “Outdoor demonstration experiment on the effect of soil albedo on soil temperature,” *Am. J. Phys.* **52**, 742–744 (1984).

⁷J. Unsworth and F. J. Duarte, “Heat diffusion in a solid sphere and Fourier theory: An elementary practical example,” *Am. J. Phys.* **47**, 981–983 (1979).

⁸H. G. Jensen, “Kohlrausch heat conductivity apparatus for intermediate or advanced laboratory,” *Am. J. Phys.* **38**, 870–874 (1970).

⁹C. H. Shaw and N. Saunders, “Intermediate laboratory experiment in heat conduction,” *Am. J. Phys.* **23**, 89–90 (1955).

¹⁰H. M. McGee, J. McInerney, and A. Harrus, “The virtual cook: Modeling heat transfer in the kitchen,” *Phys. Today* **52**(11), 30–36 (1999).

¹¹A. F. Kuckes and B. G. Thompson, *Apple II in the Laboratory* (Cambridge U.P., Cambridge, 1987), Chap. 5.

¹²B. G. Thompson and A. F. Kuckes, *IBM-PC in the Laboratory* (Cambridge U.P., Cambridge, 1992), Chap. 5.

¹³We use a National Instruments data acquisition board (USB-6210), (www.ni.com/), and MATLAB data acquisition toolbox, (www.mathworks.com/). Similar data acquisition and control systems can be used.

¹⁴D. L. Powers, *Boundary Value Problems* (Saunders College, New York, 1987).

¹⁵*A Physicist’s Desk Reference*, edited by H. L. Anderson (American Institute of Physics, New York, 1989).

¹⁶M. Jakob, *Heat Transfer* (Wiley, New York, 1949).

¹⁷*VDI Heat Atlas*, edited by E. U. Schlunder (Woodhead Publishing, Switzerland, 1993).

¹⁸Alternatively, the problem can be coded directly as shown by R. A. Kobiske and J. L. Hock, “Numerical solution to transient heat flow problems,” *Am. J. Phys.* **41**, 517–525 (1973).

¹⁹See EPAPS Document No. E-AJPIAS-76-007805 for the MATLAB code and example data. For more information on EPAPS, see <http://www.aip.org/pubservs/epaps.html>.

²⁰The op-amp in the circuit should have a FET input and be capable of single supply operation. We have substituted a TLC271A for the CA3140 with good results.

²¹We use an International Rectifier IRL530 HEXFET, which turns on with a voltage of 5 V on the gate. Others of the same series are suitable.

²²MATLAB numerical analysis software, (www.mathworks.com/).